7th Canadian Conference on Earthquake Engineering / Montreal / 1995
7ième Conférence canadienne sur le génie paraséismique / Montréal / 1995

Hysteretic Behaviour of Steel Fibre-Reinforced Concrete Frames

B.O. Katzensteiner[1] and A. Filiatrault[2]

ABSTRACT

Dynamic tests of two sets of parallel one-bay, two-storey concrete plane frames were carried out at the University of British Columbia to assess the effectiveness of steel fibre-reinforced concrete (SFRC) in seismic design. The first set of frames was constructed with a plain concrete mix and conventional steel reinforcing, while the second set was built with an SFRC mix and a modified version of the first set's reinforcing steel arrangement. The steel fibres used in the SFRC were ZP30/0.50 hooked-end, collated Dramix (Bekaert) steel fibres, and were added to the concrete at a loading of 60 kg/m^3 (0.76% by volume). Based on the hysteretic behaviour recorded during the tests, the SFRC frames appear to have performed at least as well as the conventionally-detailed frames. The more rounded shape of the SFRC hysteresis loops at maximum lateral displacement suggests that inelastic deformations of the fibres help to dissipate energy during both loading and unloading of the structure. This additional energy dissipation makes SFRC well suited for applications in seismic-resistant design.

INTRODUCTION

In ductile concrete frames designed to withstand reversing seismic loads, the joints normally contain a large percentage of reinforcing steel comprised of beam bars, column bars, and column hoops. As can be expected, placing such large quantities of steel within the confines of the beam and column formwork is labour intensive, and therefore costly. In an attempt to simplify the fabrication of these reinforcing cages and improve the inelastic performance of the concrete members, researchers such as Henager [Henager, 1974] have proposed removing some of the beam and column hoops from the joint regions, and using a fibre-reinforced instead of plain concrete mix to achieve the same confinement and ductility. The encouraging findings of this research provided the incentive for performing further dynamic tests on fibre-reinforced frames at the University of British Columbia.

CONCRETE-FRAME TEST STRUCTURES

Two structures, each consisting of two parallel, one-bay, two-storey plane frames were built for the dynamic tests. Both sets of frames were designed as part of a small office building in Vancouver, British Columbia according to the 1985 National Building Code of Canada [NBCC, 1985]. The first set was constructed with a plain concrete mix and reinforced using the Canadian concrete code [CAN3-A23.3-M84, 1985] (see Figure 1), while the second set was built with steel fibre-reinforced concrete (SFRC) and a modified version of the first set's reinforcing steel arrangement. In particular, the second

[1]Design Engineer, Sandwell Inc., Vancouver, British Columbia, V6Z 2H6.
[2]Associate Pofessor, École Polytechnique, Montréal, Québec, H3C 3A7.

set of frames had all of the confining hoops in the joints removed, along with approximately every second hoop in the beams and columns (see Figure 2). Details of the reinforcing steel layout of each set of frames is given in [Katzensteiner, 1994]. The fibres used in the concrete mix of the modified frames were ZP30/0.50 hooked-end, collated Dramix (Bekaert) steel fibres that were added to the 30 MPa concrete at a loading of 60 kg/m^3 (0.76% by volume). Both structures were loaded with concrete blocks and lead weights representing the tributary dead load plus 25% roof snow load, and instrumented with linear variable differential transformers (LVDT's), potentiometers, accelerometers, and strain gauges for recording data during the tests. Figure 3 shows the completed structure ready for testing.

TESTING PROGRAMME

The dynamic tests were divided into three phases. The first phase consisted of applying low-level excitations to the test structures and analyzing the subsequent response to determine the structure's natural frequency and damping ratio. In the second phase, each structure was subjected to an identical sequence of eight earthquake acceleration records of increasing magnitude. The third and final phase consisted of remeasuring the structure's natural frequency to assess the amount of damage that had been sustained by the frames. Results of the first and third phases of testing have been previously reported [Katzensteiner, 1994], and are not included in this paper.

The earthquake acceleration records that were applied during the second phase of testing consisted of the following:

- Tests #1 to #6: artificial Newmark-Blume-Kapur (N-B-K) earthquake scaled to peak ground accelerations of 0.03*g*, 0.07*g*, 0.14*g*, 0.18*g*, 0.32*g*, and 0.35*g* (*g* is the acceleration due to gravity).
- Test #7: 1989 Loma Prieta (Oakland Wharf) earthquake scaled to 0.27*g*.
- Test #8: artificial Vancouver subduction-type earthquake scaled to 0.26*g*.

The above magnitudes represent the average of the actual peak ground accelerations of the two structures during a given test. Each average varies by no more than 0.02*g* from the peak accelerations recorded during that particular test. It should be noted that the above set of accelerations are not identical to the set reported in [Katzensteiner, 1994], since the latter accelerations were target values rather than actual recorded values. This discrepancy, however, is purely a matter of how the acceleration values are reported.

CALCULATION OF HYSTERETIC BEHAVIOUR DURING SEISMIC TESTS

To examine the hysteretic behaviour of the two test structures, force–deflection plots were constructed from the data collected during each of the eight seismic tests. These plots are shown in Figures 4 to 19, all of which are drawn to the same scale to aid comparison of the results. In these plots, the base shear $V(t)$ is calculated from:

$$V(t) = m_1 a_1(t) + m_2 a_2(t)$$

where m_1 = tributary mass at level of lower beams (5992 kg)
m_2 = tributary mass at level of upper beams (4862 kg)
$a_1(t)$, $a_2(t)$ = absolute acceleration of structure at level of lower and upper beams, respectively, at time t

The acceleration–time histories $a_1(t)$ and $a_2(t)$ were provided by the two accelerometers that were attached to the lower and upper joint of one frame. The relative lateral displacement $x_{REL}(t)$ is computed from the difference of the absolute lateral displacement–time history of the joints recorded by the potentiometer units and the absolute ground motion recorded by the shaking table's LVDT:

$$x_{REL}(t) = x(t) - x_G(t)$$

where $x_{REL}(t)$ = relative lateral displacement of joint at time t
$x(t)$ = absolute lateral displacement of joint at time t
$x_G(t)$ = absolute lateral displacment of ground at time t

DISCUSSION & CONCLUSIONS

Examining Figures 4 to 19 shows the size of the hysteresis loops to increase as successively larger earthquakes are applied, indicating that more energy is absorbed through inelastic action of the beams and columns. Both test structures responded in an essentially elastic manner during the first three low-magnitude tests, as evidenced by the primarily linear relationship of the hysteretic loops. It can also be seen that the stiffness of the structures, which is equal to the slope of the hysteresis loops, gradually decreases over the course of the seismic testing programme as the frames become more heavily damaged.

Two significant observations can be made with regard to the hysteretic plots shown in the figures. Comparing the area enclosed by hysteresis loops of equal relative lateral displacements shows the SFRC frames to have absorbed at least as much energy per dynamic cycle as the conventionally-detailed frames. From this qualitative comparison, it would therefore appear that the SFRC frames performed as well as the conventional frames during the seismic tests. The other significant observation of the hysteretic plots is that the shape of the SFRC hysteresis loops at maximum lateral displacement is more rounded than the loops of the conventional frames, even for the low-magnitude N-B-K tests (see Figures 9 and 11). This behaviour suggests that the fibres in the tension faces of the beams and columns dissipate energy during both loading and unloading of the structure. During loading, energy is dissipated by fibres yielding and pulling out of the concrete matrix as tension cracks open. These yielded and dislodged fibres in turn provide resistance during unloading as the structure accelerates in the opposite direction, and energy is thus expended as fibres are buckled and pushed back into the concrete matrix. This additional energy dissipation makes SFRC well suited for applications in seismic-resistant construction.

REFERENCES

CAN3-A23.3-M84, *Design of Concrete Structures for Buildings*, Canadian Standards Association, Toronto, 1985.

Henager, C.H., **"Steel Fibrous, Ductile Concrete Joint for Seismic-Resistant Structures,"** *Reinforced Concrete Structures in Seismic Zones*, SP-53, American Concrete Institute, Detroit, 1974.

Katzensteiner, B., Mindess, S., Filiatrault, A., Banthia, N., **"Dynamic Tests of Steel-Fiber Reinforced Concrete Frames,"** *Concrete International*, V.16, No.9, American Concrete Institute, Detroit, 1994.

NBCC 1985, **"Structural Design,"** Part 4, *National Building Code of Canada 1985*, National Research Council of Canada, Ottawa, 1985.

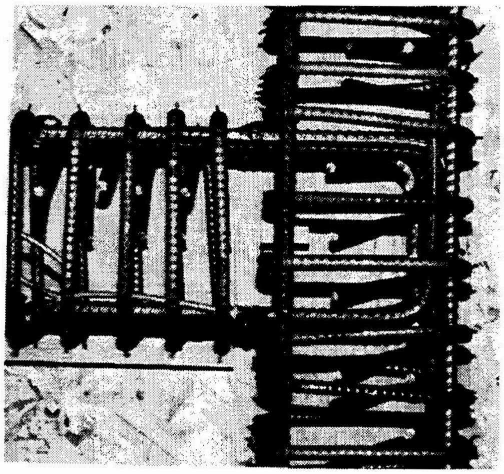

Figure 1: Reinforcing Steel of Conventional Frames

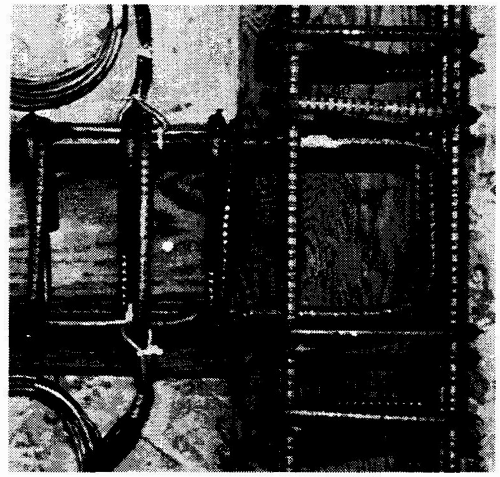

Figure 2: Reinforcing Steel of SFRC Frames

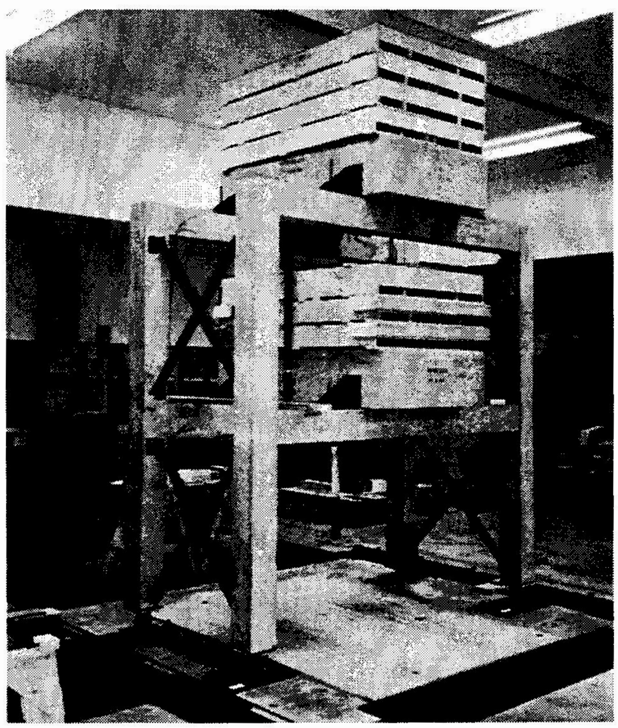

Figure 3: Completed Structure Prior to Testing

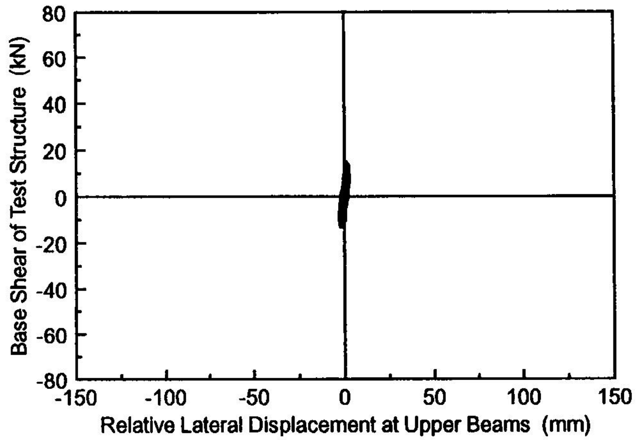

Figure 4: Conventional Frames, Test #1 (0.03g N-B-K)

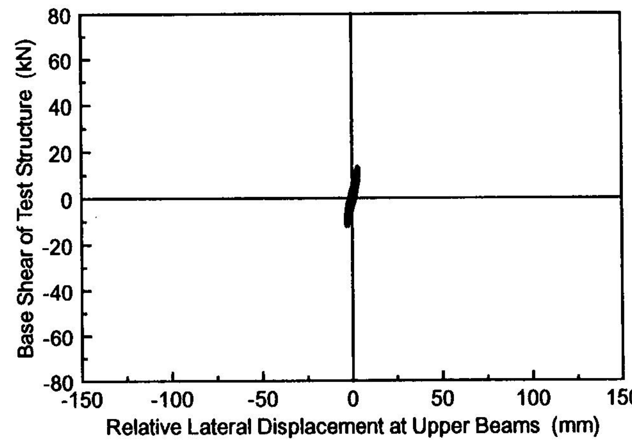

Figure 5: SFRC Frames, Test #1 (0.03g N-B-K)

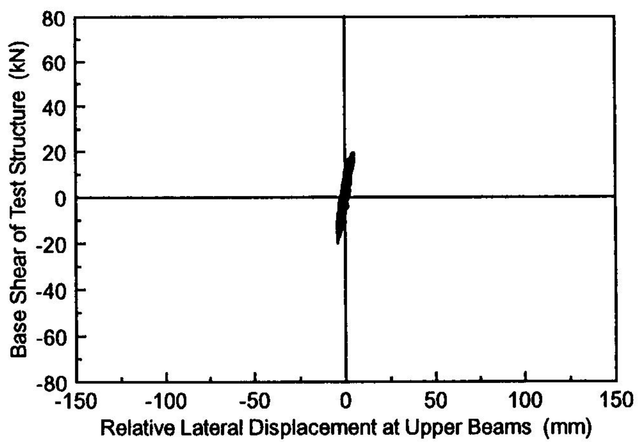

Figure 6: Conventional Frames, Test #2 (0.07g N-B-K)

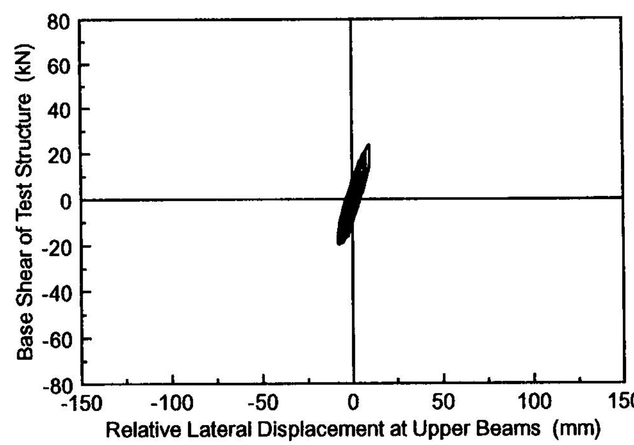

Figure 7: SFRC Frames, Test #2 (0.07g N-B-K)

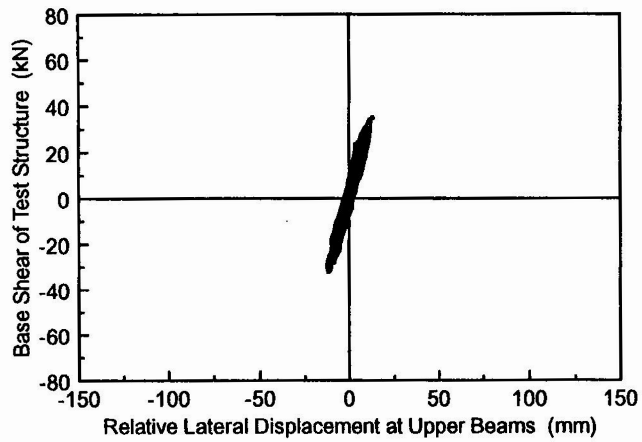

Figure 8: Conventional Frames, Test #3 (0.14*g* N-B-K)

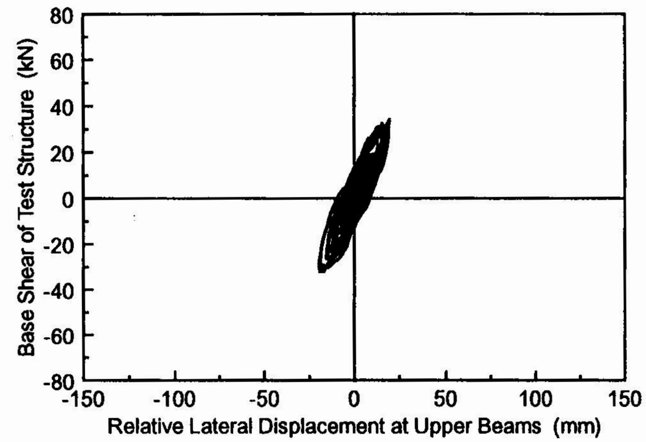

Figure 9: SFRC Frames, Test #3 (0.14*g* N-B-K)

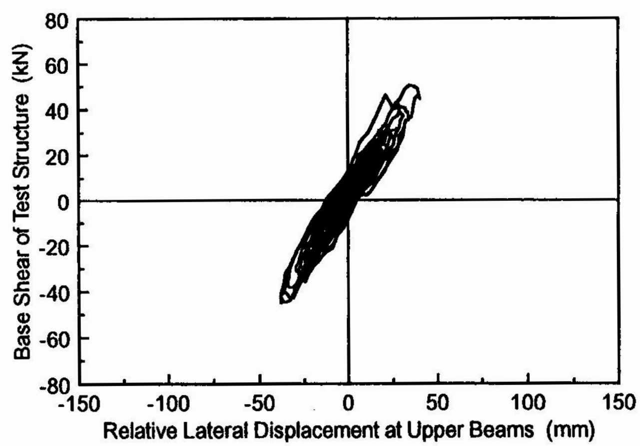

Figure 10: Conventional Frames, Test #4 (0.18*g* N-B-K)

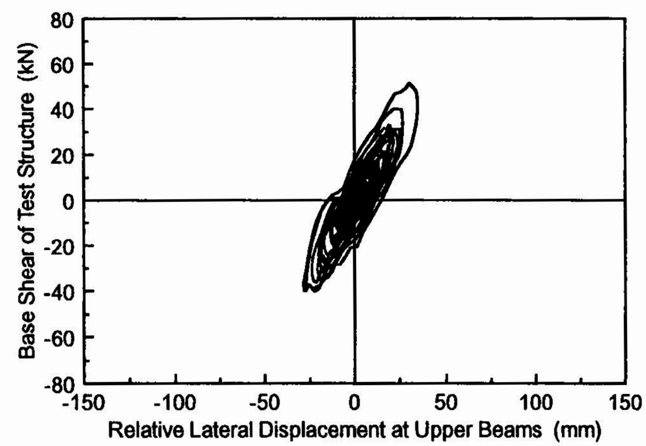

Figure 11: SFRC Frames, Test #4 (0.18*g* N-B-K)

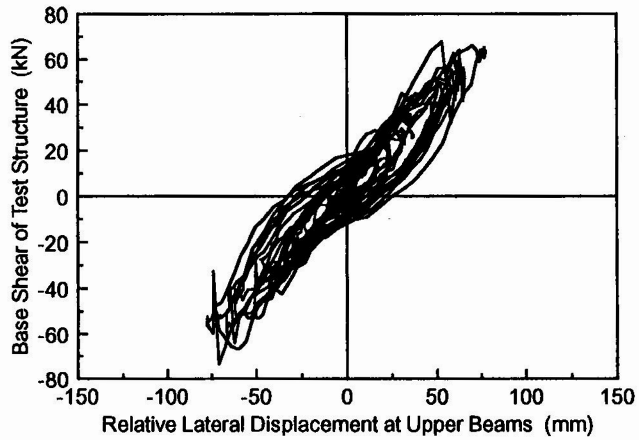

Figure 12: Conventional Frames, Test #5 (0.32*g* N-B-K)

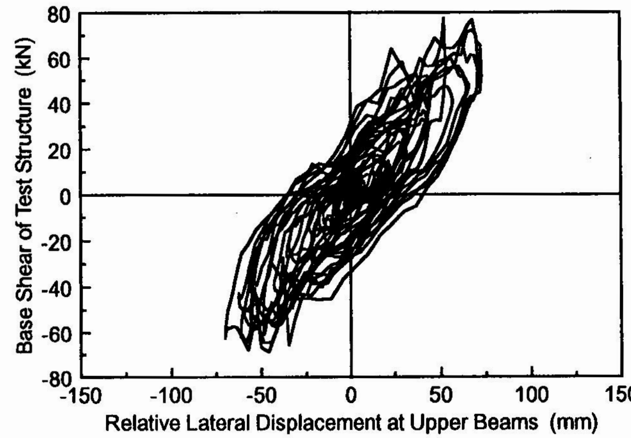

Figure 13: SFRC Frames, Test #5 (0.32*g* N-B-K)

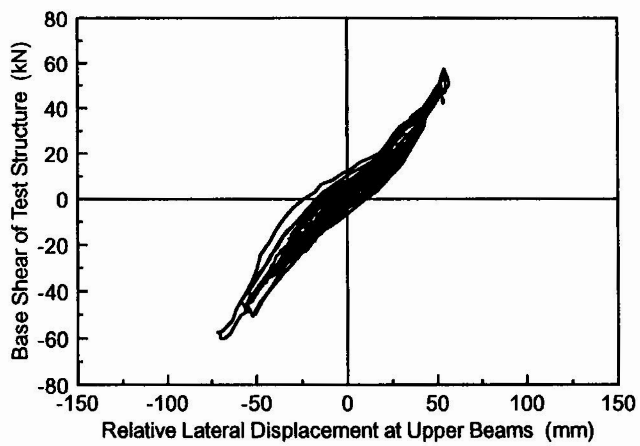

Figure 14: Conventional Frames, Test #6 (0.35*g* N-B-K)

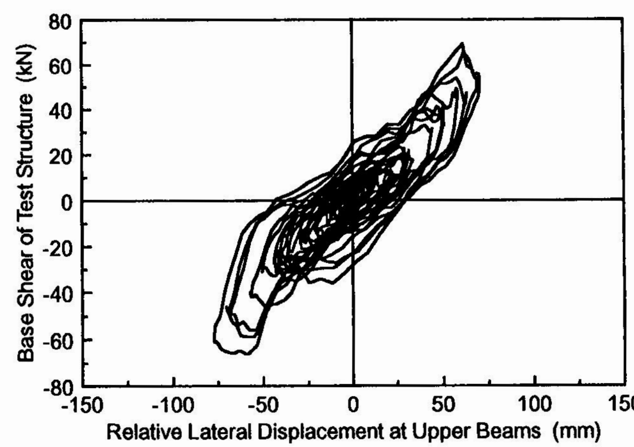

Figure 15: SFRC Frames, Test #6 (0.35*g* N-B-K)

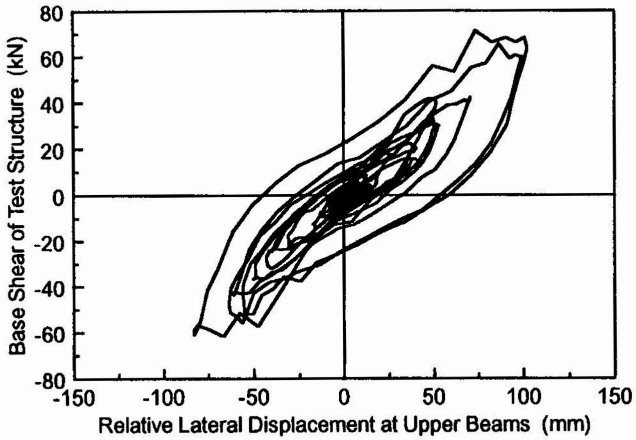

Figure 16: Conventional Frames, Test #7 (0.27*g* Loma Prieta)

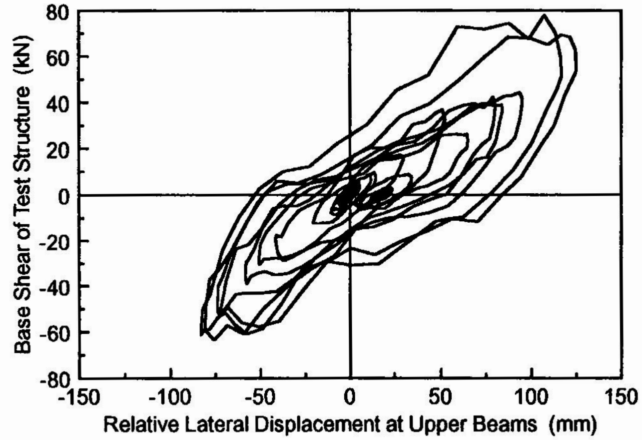

Figure 17: SFRC Frames, Test #7 (0.27*g* Loma Prieta)

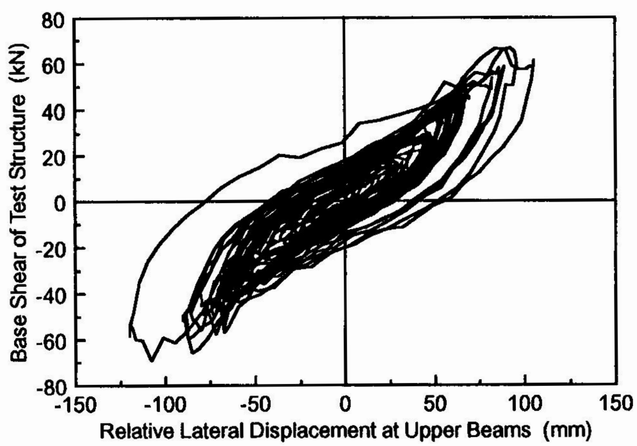

Figure 18: Conventional Frames, Test #8 (0.26*g* Subduction)

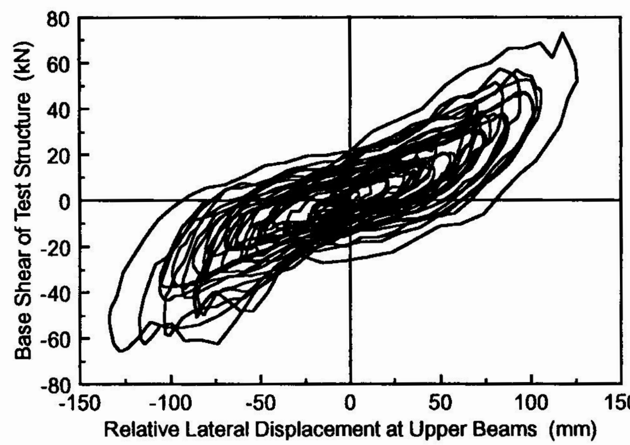

Figure 19: SFRC Frames, Test #8 (0.26*g* Subduction)